





Article

Backhaul-Aware Dimensioning and Planning of Millimeter-Wave Small Cell Networks

Pablo Muñoz ^{1,2,*} , Oscar Adamuz-Hinojosa ^{1,2} , Pablo Ameigeiras ^{1,2},
Jorge Navarro-Ortiz ^{1,2}  and Juan J. Ramos-Muñoz ^{1,2} 

¹ Department of Signal Theory, Telematics and Communications, University of Granada, 18071 Granada, Spain; oadamuz@ugr.es (O.A.-H.); pameigeiras@ugr.es (P.A.); jorgenavarro@ugr.es (J.N.-O.); jjramos@ugr.es (J.J.R.-M.)

² Research Center on Information and Communication Technologies, University of Granada, 18014 Granada, Spain

* Correspondence: pabloml@ugr.es; Tel.: +34-958248876

Received: 6 August 2020; Accepted: 29 August 2020; Published: 2 September 2020



Abstract: The massive deployment of Small Cells (SCs) is increasingly being adopted by mobile operators to face the exponentially growing traffic demand. Using the millimeter-wave (mmWave) band in the access and backhaul networks will be key to provide the capacity that meets such demand. However, dimensioning and planning have become complex tasks, because the capacity requirements for mmWave links can significantly vary with the SC location. In this work, we address the problem of SC planning considering the backhaul constraints, assuming that a line-of-sight (LOS) between the nodes is required to reliably support the traffic demand. Such a LOS condition reduces the set of potential site locations. Simulation results show that, under certain conditions, the proposed algorithm is effective in finding solutions and strongly efficient in computational cost when compared to exhaustive search approaches.

Keywords: cell planning; Fifth Generation; Small Cells; Heterogeneous Networks; millimeter-wave

1. Introduction

The deployment of the Fifth Generation (5G) of mobile communications has recently started, and it is envisaged to have a great impact on the digital society. In addition to the speed improvement of mobile broadband services, 5G will allow the definitive launch of massive machine communications and mission-critical machine communications [1,2]. The new services may require up to 10 Gbps peak data rate, 1000 times the bandwidth per unit area, up to 100 times the devices connected simultaneously, low latency (down to 1 ms), ultra-high reliability (up to 99.999% availability) and low power consumption (up to 10-year battery life). The use of high-band spectrum, virtualization, edge computing and network slicing are the main pillars of the unprecedented technological renewal required for current access, backhaul (BH) and core networks [3,4].

To cope with the explosive growth in demand for bandwidth, network densification using millimeter-wave (mmWave) Small Cells (SCs) is considered a key enabler of 5G systems [5,6]. SCs are short-range, low-cost, low-power base stations that provide additional capacity and extended coverage to the traditional macro-only cellular network. With dense SC deployments, the whole system throughput can be enhanced by increasing the frequency reuse. However, densifying the access network affects the BH network, which should be re-designed to avoid performance bottleneck, management complexity and high costs to the infrastructure provider [7]. While connecting SCs to the BH via optical fiber may result too expensive (e.g., in sparsely located fiber access areas), mmWave communications are an attractive alternative for supporting high bandwidth BH connections [8,9]. They can be established

either to the macro base stations, which are normally backhauled by high-capacity wired links (e.g., fiber), or to other SCs that would act as relays. Wireless backhaul is a cost-effective solution to provide coverage in public or private venues, especially in the context of industrial environments (e.g., mining facilities, ports, etc.).

The mmWave band is defined as spectrum between 30 and 300 GHz. It provides large amounts of bandwidth compared to the currently congested sub-6 GHz spectrum. Nevertheless, mmWave is affected by higher propagation and penetration losses than the sub-6 GHz bands. Thus, a line-of-sight (LOS) communication path with highly directional beams and high-gain antennas is required to achieve several gigabits per second [10]. Thanks to the recent advancement in hardware design, this can be realized with massive MIMO implementations using a large number of very low power antennas [11,12]. MIMO beamforming has the benefit of reduced inter-antenna interference due to the high directivity of the individual links. Accordingly, mmWave and massive MIMO technologies can be jointly applied to the BH network in order to enhance the overall performance of the cellular system [13].

In the context of large-scale mmWave SC deployments, there are new challenges to tackle. One of the biggest challenges is how to strategically locate and configure the SCs to provide the required capacity and coverage while minimizing roll-out costs. This problem, known as cellular planning, has been widely investigated in traditional scenarios. For macrocell (MC) networks, the common approach is based on analyzing demand and service coverage requirements [14]. With the advent of Heterogeneous Networks (HetNets), the focus is on mitigating the cross-tier interference between MCs and SCs [15,16]. More recently, the optimal placement and minimization of base stations using mmWave is studied in several works. Specifically, in [17], a meta-heuristic algorithm based on swarm intelligence is proposed to optimally locate base stations, while an iterative method is applied to remove base stations that are redundant. In [18], a more generic analysis is done for cellular planning, considering the main constraints of coverage, capacity and cost for high-capacity scenarios. The joint base station placement and beam steering problem is analyzed in [19], where the mmWave network coverage is optimized within hotspots and in-venue regions. A typical assumption is that the capacity in the access network is not limited by the BH. There are few works addressing the lack of capacity in the BH based on whether wired [20] or wireless [7,21] solutions are employed. In dense deployments, the wired solutions may not be scalable to support the large number of SCs. Deploying wired links to a cell site also involves long roll-out times requiring permission and costly activities such as trenching, boring or ducting [4]. Regarding wireless BH solutions, mobile operators are considering the use of mmWave in the V-band (60 GHz) and the E-band (70/80 GHz), which are appropriate to support 5G due to their 10–25 Gbps data rates. However, because of the higher frequencies, these bands are prone to atmospheric effects or rain fade, which can attenuate the signal and limit its range. Thus, the wireless option presents more challenging issues to face, such as the directional LOS design [22], the self-BH [23–25] or the multi-hop BH [26–28]. The in-band self-BH problem is aimed at finding the optimal BH and access time resource partition, combined with the user association and the beam alignment. In ultra-dense networks, the multi-hop design allows mitigating the impact of locally intensive traffic, while simultaneous multi-hop backhaul connections can also reduce the link outages due to blockage. This issue, together with the optimization of energy consumption, is addressed in [27], where the base stations in light-load condition are turned off to minimize power consumption. Both works [27,28] employ Software-Defined Networks (SDN) technology for dynamic construction of mesh networks in order to handle the variations of the traffic load. The multi-hop BH in multi-operator scenarios is addressed in [29], where a matching theory-based algorithm is developed considering both wireless channel characteristics and economic factors. In [30,31], the multi-hop BH is analyzed for scenarios including mobile base stations. In the case of [31], they are aerial base stations, which offer better LOS channels compared to the terrestrial ones.

There are also key features in 5G such as multi-tenancy that steer cellular planning to work with a more automated, flexible and agile infrastructure than in previous generations. In [32], the authors

proposed a self-planning framework to update the cellular infrastructure in response to various events such as the deployment of a new tenant's slice (i.e., an isolated logical network). The cell deployment should be accompanied with intelligent resource scheduling and allocation in the BH to provide optimal network performance. In this line, the work in [33] proposes an optimization algorithm for steering data traffic of multiple slices in the BH.

Despite the existence of relevant work on cellular planning, the consideration of key 5G enablers (e.g., mmWave, massive MIMO, wireless BH, multi-tenancy, etc.) is scattered in the literature. Most of the above-mentioned works either address the planning problem in the access network (i.e., determine the cell location) or they attack problems in the BH network, such as routing and spectrum usage. The combination of these two problems is not sufficiently addressed. Although there are some proposals in the literature [7,21], their formulation neglects key considerations such as the multi-hop capability in the BH network. In addition, the spatial traffic distribution models used for performance evaluation are unlikely in reality.

In this work, we tackle the SC planning problem under two major assumptions: (i) SCs are wirelessly backhauled via the SC and/or MC layer; and (ii) a self-planning framework enables incremental deployment on top of the existing infrastructure. Unlike previous works, the first hypothesis implies two constraints at the same time: a maximum number of backhauled SCs per node and a maximum number of hops until reaching the MC. The second hypothesis allows considering a more realistic scenario, where a HetNet infrastructure is available to support the deployment of the new SCs. The main contributions of this work are as follows. We formulate it as a mixed integer non-linear programming problem, considering several key conditions that have not previously been considered together, such as the required LOS between nodes, the maximum number of hops, the number of simultaneous BH links and the number of SCs backhauled by every node. Then, we present an iterative two-step algorithm to solve the problem with limited complexity. The consideration of computationally-efficient methods is relevant since the wireless BH solutions have significantly lower associated time-to-deploy than wired options. In a first step, the heuristic algorithm provides an initial solution for satisfying the user demand. In a second step, the algorithm refines the solution to adapt it to the BH constraints. For the evaluation, we utilized standard models from 3GPP and a practical interference model for mmWave beamforming. The evaluation was carried out for different MC densities in the area of interest to establish various BH conditions that affect the behavior of the planning algorithm. In addition, a sensitivity analysis of the BH antenna gain as a key radio parameter was performed to study its effect on spectral efficiency. Simulation results show that the proposed algorithm can provide effective solutions with reduced computational costs and comparable performance to brute-force search approaches. This low complexity can ensure its application to large-scale scenarios. Moreover, the algorithm can easily be integrated with existing commercial planning tools, which usually combine live network measurements with predictions for accurate network planning.

The remainder of this paper is organized as follows. Section 2 starts with the system model and the formulation of the BH-aware cell dimensioning and planning problem. Section 3 describes the proposed computationally-efficient method considering both user demands and BH constraints. In Section 4, after describing the simulation scenario and setup, the performance of the proposed method is evaluated. Finally, Section 5 provides some concluding remarks.

2. System Model and Problem Description

2.1. System Model

Consider a two-tier HetNet scenario consisting of a set $B = B_M \cup B_S$ of base stations, where B_M are the MCs and B_S are the SCs, all managed by a certain operator. The access network serves a set U of user equipments (UEs), each demanding a capacity of D_u . The sub-6 GHz and mmWave bands are used for access transmissions in MCs and SCs, respectively. In the BH network, each MC has a high-speed

optical fiber connection, while each SC j can connect either to another SC or directly to a MC using an mmWave LOS link with a capacity C_j^{BH} . In this way, the SCs can act as aggregator nodes to relay UE data. The required LOS between the access and BH nodes limits the area of interest to a set S_b^{LOS} of candidate sites for placing the SC b . The spectrum in the access network is organized in resource blocks (RBs) that are allocated to the nodes in a semi-persistent manner to meet current demands [21]. Each UE u is allocated a fraction W_u of the spectrum allocated to its serving node. Non-overlapped mmWave spectrum in the V-band is allocated for access and BH networks. The V-band is selected because of its unlicensed or lightly licensed spectrum use. Due to the attenuation effects of oxygen absorption, this band can be effectively used to connect closely spaced SCs with short links that are daisy-chained and aggregated for transport to the network core [4]. Let W^{BH} be the bandwidth dedicated to the BH in each node. Beamforming is employed in the BH network to enable simultaneous transmissions (beams) to different nodes using the same RBs. However, SCs acting as relays in a multi-hop BH link will use time or frequency multiplexing for transmissions with the nodes at the previous and next hops. The SCs can communicate directly with the other nodes through the X2 protocol, which is an ultra-fast broadband-related protocol that allows mobile operators to use different topologies to offload traffic.

For the access network, suppose that a UE u is served by certain node b . Let $\gamma_{u,r}$ be the Signal-to-Interference-plus-Noise Ratio (SINR) of this UE when transmitting on the RB r , defined as:

$$\gamma_{u,r} = \frac{p_{u,b}^{RX}}{\left(\sum_{j \in B_I \setminus \{b\}} L_j \cdot \pi_{j,r} \cdot p_{u,j}^{RX} \right) + p_N}, \tag{1}$$

where $p_{u,b}^{RX}$ is the received power by the UE u from the node b , L_j is the cell load factor of the node j , $\pi_{j,r}$ is a function that takes the value 1 when the RB r is allocated to the node j and the value 0 otherwise, I can take the value of M or S depending on the cell type (i.e., MC or SC) and p_N is the noise power measured in one RB. The cell load factor is defined as the relation between the service demand and cell capacity according to the work in [32]. The spectral efficiency $SE_{u,r}$ of the UE u in the RB r is calculated from the $\gamma_{u,r}$ based on the following SINR mapping [34]:

$$SE_{u,r} = \begin{cases} 0 & , \quad \gamma_{u,r} < \gamma_{min} \\ \rho \cdot \log_2(1 + \gamma_{u,r}) & , \quad \gamma_{min} \leq \gamma_{u,r} < \gamma_{max} \\ SE_{max} & , \quad \gamma_{u,r} \geq \gamma_{max} \end{cases} \tag{2}$$

where SE_{max} is the maximum achievable spectral efficiency with link adaptation; γ_{min} and γ_{max} are the minimum and maximum SINR values, respectively; and ρ specifies the attenuation factor, which represents implementation losses. The capacity offered by the node b to the UE u is expressed as:

$$C_u = \frac{W_u}{|R_b|} \cdot \sum_{r \in R_b} SE_{u,r} \tag{3}$$

where R_b is the subset of RBs allocated to the serving node b . The fraction W_u allocated to the UE depends on the resource scheduling scheme. For example, assuming a round-robin scheme, it is given by:

$$W_u = \frac{W_{RB} \cdot |R_b|}{|U_b|}, \tag{4}$$

where W_{RB} is the spectral occupancy of a RB (e.g., 180 kHz assuming a subcarrier spacing of 15 kHz) and U_b is the subset of UEs served by the same node b .

For the BH network, the SCs are equipped with directional antennas whose gain pattern is modeled as in [35]:

$$A_b(\theta) = \begin{cases} A_{max} & , \quad |\theta| \leq \theta^m \\ A_{min} & , \quad \text{otherwise} \end{cases} \tag{5}$$

where θ^m is the main-lobe width and A_{max} and A_{min} are the main and side-lobe gains, respectively. The antenna beams in the BH are aligned, so that the effective gain on BH links is A^2_{max} . Each candidate SC location in the area of interest has a probability of LOS propagation from a given BH node. This probability is taken from the 3GPP models in [36], which are applicable to frequencies up to 100 GHz. Unlike what happens with the UEs in the access links, an improvement of the LOS probability is applied to the BH links due to the local planning activities. According to the model presented in [37], the LOS probability p' after local planning optimization is determined as follows:

$$p' = 1 - (1 - p)^\tau, \tag{6}$$

where p is the LOS probability without local planning optimization calculated as in [36] and τ is a parameter that depends on the site planning searching radius (e.g., $\tau = 3.1$ for 50-m radius). In addition, the LOS/NLOS conditions at multiple positions are also correlated to provide spatial consistency. Following the model in [38], the correlated LOS/NLOS conditions are generated by applying an exponential spatial filter to the independent random values with a given correlation distance (e.g., 50 m for 3GPP urban macro and micro scenarios [36]):

$$\tilde{v}_{c_x,c_y} = \sum_{m=1}^M \sum_{n=1}^N v_{c_x,c_y} \exp\left(-\frac{d_E(s_{c_x,c_y}, s_{c_m,c_n})}{\Delta d}\right), \tag{7}$$

where v_{c_x,c_y} and \tilde{v}_{c_x,c_y} are the independent and correlated LOS visibility variables, respectively, in the location (c_x, c_y) , where c_x and c_y are the x - and y -coordinates. The parameter Δd represents the correlation distance, d_E stands for the Euclidean distance and $M \times N$ is the total number of grid points that are considered in the area of interest. Since the independent LOS visibility variable is Boolean to represent LOS and NLOS states, the obtained value of the correlated variable is rounded to the nearest 0 or 1. From this information, the set S_b^{LOS} of candidate sites for placing an SC can be obtained. The same exponential spatial filter is also applied to the shadow fading in order to provide spatial consistency.

The SINR experienced by the SC b when served by its BH node h^b is determined as:

$$\gamma_b^{BH} = \frac{p_{h^b}^{TX} \cdot A_{max}^2 \cdot G_{h^b,b}^{BH}}{\left(\sum_{j \in B_S | j \neq b, h^j \neq h^b} L_{h^j}^{BH} \cdot p_{h^j}^{TX} \cdot A_{h^j}(\theta_b) \cdot A_b(\theta_{h^j}) \cdot G_{h^j,b}^{BH} \right) + p_N^{BH}}, \tag{8}$$

where $p_{h^b}^{TX}$ is the transmit power of the BH node h^b ; $G_{h^b,b}^{BH}$ is the channel gain (i.e., path loss and shadow fading) between the SC and its BH node; $L_{h^j}^{BH}$ represents the cell load factor of the BH node h^j ; $A_{h^j}(\theta_b)$ and $A_b(\theta_{h^j})$ are the transmitter and receiver antenna gains in the direction determined by the nodes b and h^j , respectively; and p_N^{BH} stands for the noise power measured in the bandwidth of the BH network, W^{BH} . Note that this expression assumes a single polarized MIMO system. Although cross-polarization helps reduce the undesired radio interference, it requires the use of special antennas and is more sensitive to interference and rain [39]. The cell load factor of BH nodes is given by the traffic load of their served SCs, connected with either direct or multi-hop links. The spectral efficiency SE_b^{BH} of the SC b is obtained using Equation (2). Lastly, the corresponding capacity C_b^{BH} offered by this SC is determined as:

$$C_b^{BH} = W^{BH} \cdot SE_b^{BH}. \tag{9}$$

The operator offers the network infrastructure to multiple tenants. With the aim of satisfying the highly diversified radio access needs in space and time of these tenants, we adopt the self-planning framework presented in [32]. Under this framework, the aggregated UE demand and actual network capacity are compared to trigger particular planning actions such as deploying new SCs or reallocating the available spectrum.

2.2. Problem Description

In our problem formulation, we assume an existing infrastructure formed by a set $B_0 = B_{M,0} \cup B_{S,0}$ of base stations that has previously been deployed in certain locations s_{b0} , where $b_0 \in B_0$ stands for the node. We define the variable $z_s^{SC} \in \{0,1\}$ at location $s \in S$ to indicate with value 1 that an SC is deployed there. Likewise, $z_s^{MC} \in \{0,1\}$ indicates the locations of the MCs. The variable $x_{i,j} \in \{0,1\}$ specifies that the node i is backhauled via the node j and $y_{u,j} \in \{0,1\}$ indicates that the UE u is served by the node j . For simplicity, we consider that the cell sizes and maximum distance for BH link availability are such that any SC can be backhauled to the MC through one SC at most, which implies the multi-hop BH link to be limited to two hops. In addition, the problem is focused on the downlink because of the asymmetric nature of data traffic. Given this, the SC dimensioning and planning problem can be expressed as follows:

$$\min_{z_s^{SC}, x_{i,j}} |B_S|, \tag{10}$$

subject to

$$\alpha D_u \leq C_u \quad \forall u \in U, \tag{11}$$

$$\beta \left(\sum_{u \in U} y_{u,j} D_u + \sum_{i \in B_S} x_{i,j} \sum_{u \in U} y_{u,i} D_u \right) \leq C_j^{BH} \quad \forall j \in B_S, \tag{12}$$

$$x_{i,j} + x_{j,k} + x_{k,l} \leq 2 \quad \forall i, j, k, l \in B, \tag{13}$$

$$\sum_{i \in B_S} x_{i,j} \leq N_S \quad \forall j \in B_S, \tag{14}$$

$$x_{i,j} + x_{j,i} \leq 1 \quad \forall i, j \in B_S, \tag{15}$$

$$\sum_{j \in B} x_{i,j} = 1 \quad \forall i \in B_S, \tag{16}$$

$$\sum_{j \in B} y_{u,j} = 1 \quad \forall u \in U, \tag{17}$$

$$z_{s_j}^{SC} = 1 \quad \forall j \in B_{S,0}, \tag{18}$$

$$z_{s_j}^{MC} = 1 \quad \forall j \in B_{M,0}, \tag{19}$$

where α and β are parameters to adjust the required user throughput in the network and N_S is the maximum number of SCs that can be backhauled by a certain SC. The objective is to minimize the deployment cost (i.e., the number of newly deployed SCs) while guaranteeing the UE demands. In classical cellular planning, the deployment of new base stations is motivated by the insufficient quality of the radio links between the UEs and the base stations. In this way, Equation (11) represents the quality of service in the access network, unifying both coverage and capacity constraints for the UEs.

The cellular planning problem with wireless BH requires the consideration of a set of constraints. In particular, Equation (12) denotes the BH capacity constraint, which implies that an SC acting as relay aggregates the traffic from its backhauled SCs to that from its served UEs. Equation (13) establishes that the multi-hop BH link is limited to a maximum number of hops. Exceeding this condition may cause higher delays due to the processing time at each node. Equation (14) limits the number of SCs backhauled by one node. This condition help avoid the congestion of links in the BH network. With Equation (15), two SCs cannot be mutually assigned as their BH nodes. Breaking this condition would create undesirable loops in the BH network. Equations (16) and (17) ensure that every SC (UE) is backhauled (served) by exactly one node. Multiple links from the same SC can be used for load balancing or redundancy purposes. However, for simplicity, such objectives are out of the scope of this paper. Finally, Equations (18) and (19) represent the initial set of deployed SCs and MCs whose

locations must remain fixed. As previously stated, this represents a realistic assumption for HetNets, where the current infrastructure is insufficient to cope with the increasing demand.

3. Proposed Dimensioning and Planning Algorithm

The formulated problem for cellular dimensioning and planning under non-ideal BH conditions is a mixed integer non-linear program. Thus, our proposed solution is a computationally-efficient BH-aware (CEBA) algorithm that follows the heuristic approach described in Algorithms 1 and 2, where the variable h^b indicates the BH node for the node b and p_b^{RX} is the received power from b . The UE demand D_u is expressed as traffic density, with $d_{x,y}$ representing the traffic demand in the grid point (c_x, c_y) . The function $F(\cdot)$ is a filter to smooth the traffic demand variable. Dimensioning is based on iteratively adding a new SC to the planning problem until the network (both access and BH) capacity is enough to satisfy the UE demands (Steps 2–3 in Algorithm 1). The planning problem, where the number of SCs is invariant, is divided into two stages: the first aims at optimally placing the SCs based on the UE demands (Steps 4–7 in Algorithm 1), while the second further optimizes the location of the SCs to satisfy the required capacity in the BH links (Algorithm 2).

Algorithm 1 CEBA dimensioning and planning algorithm

Input: initial solution: $\mathbf{q}_0 = [\mathbf{x}, \mathbf{z}^{\text{SC}}, B_{S,0}; \mathbf{z}^{\text{MC}}, B_{M,0}, D_u, N_S, \alpha, \beta$

- 1: initialize $\mathbf{q} \leftarrow \mathbf{q}_0, B_S \leftarrow B_{S,0}$
- 2: **while** constraints in (11) or (12) are not met
- 3: add a new SC, $|B_S| \leftarrow |B_S| + 1$
- 4: use k -means to partition $\omega = (c_x, c_y, F(d_{x,y}))$ in $|B_S|$ clusters and obtain centroids $s_b, b \in B_S$
- 5: optimize s_b by applying the steepest-ascent method n times to the function $F(d_{x,y})$
- 6: select $|B_{S,0}|$ elements $b \in B_S$ having the smallest $d_E(s_b, s_{b_0})$ and replace them by $b_0 \in B_{S,0}, B_{S,0} \subset B_S$;
- 7: update $s_b, \mathbf{z}^{\text{SC}}$
- 7: assign BH node to each $b \in B_S$: $h^b = \arg_c \max p_c^{RX}$ with $c \in B_M$ and $s_b \in S_c^{LOS}$; if not possible, try with $c \in B_S$ only if c has LOS BH with 1-hop link; update \mathbf{x}
- 8: **if** $\exists b \in B_S \mid b$ has NLOS BH or b does not satisfy (14) **then**
- 9: execute Algorithm 2, backhaul-aware optimization
- 10: **end if**
- 11: **end while**

Output: optimized \mathbf{q} and B_S

The planning based on UE demands serves to increase the SC deployment in areas where the demand is high, making the cell size smaller. Following this principle, the k -means algorithm is first applied to identify high- and low-traffic subareas, resulting in a set of centroids as initial candidate locations for the SCs. The filter $F(\cdot)$ serves to remove irrelevant, small peaks of the traffic demand distribution before applying the k -means algorithm. The solution is refined through the steepest-ascent method to bring the SCs closer to the high-traffic subareas, achieving better spectral efficiency. Then, the location of some SCs are adjusted to match the location of the currently deployed SCs based on the minimum distance to them. With respect to parameter settings, the transmit power is set to have $\gamma = 9$ dB at $\sqrt{3}/2$ of the inter-site distance [32]. The number of RBs allocated to each SC is set to be proportional to the UE demand, and the RB selection is made as in [32] to reduce inter-cell interference.

Algorithm 2 Backhaul-aware optimization algorithm

Input: $\mathbf{q} = [\mathbf{x}, \mathbf{z}^{\text{SC}}], B, \{s_b\}, N_S$

- 1: **for** $b \in B_S$
- 2: **if** b has NLOS BH **then**
- 3: create a set C of candidate BH nodes: $C \leftarrow B \setminus \{b, \text{nodes with NLOS BH or 2-hop BH link}\}$
- 4: **for** $c \in C$
- 5: given the locations $s_c^{\text{LOS}} \in S_c^{\text{LOS}}$ having LOS with c , calculate: $\hat{s}_c^{\text{LOS}} = \arg s_c^{\text{LOS}} \min d_E(s_b, s_c^{\text{LOS}})$
- 6: **end for**
- 7: set BH node for b : $h^b = \arg_c \min d_E(s_b, \hat{s}_c^{\text{LOS}})$, update \mathbf{x}
- 8: set location: $s_b = \hat{s}_{h^b}^{\text{LOS}}$, update \mathbf{z}^{SC}
- 9: **end if**
- 10: **end for**
- 11: **for** $b \in B_S$
- 12: **if** constraint in (14) is not met for b **then**
- 13: create a set G of SCs backhauled by b
- 14: **for** $g \in G$
- 15: create a set C of candidate BH nodes: $C \leftarrow B \setminus \{b, g, \text{nodes with NLOS BH or 2-hop BH link}\}$
- 16: **for** $c \in C$
- 17: given the locations $s_c^{\text{LOS}} \in S_c^{\text{LOS}}$ having LOS with c , calculate: $\hat{s}_c^{\text{LOS}} = \arg s_c^{\text{LOS}} \min d_E(s_g, s_c^{\text{LOS}})$
- 18: **end for**
- 19: calculate: $h^g = \arg_c \min d_E(s_g, \hat{s}_c^{\text{LOS}})$, $r^g = d_E(s_g, \hat{s}_{h^g}^{\text{LOS}})$
- 20: **end for**
- 21: **sort** $g \in G$ by r^g in descending order with new index g'
- 22: **for** $g' \in G$
- 23: **if** constraint in Equation (14) is met for $h^{g'}$ **then**
- 24: set $s_{g'} = \hat{s}_{h^{g'}}^{\text{LOS}}$, update \mathbf{z}^{SC}
- 25: set $h^{g'}$ as BH node for g' , update \mathbf{x}
- 26: **end if**
- 27: **if** constraint in (14) is met for b **then**
- 28: **break**
- 29: **end if**
- 30: **end for**
- 31: **end if**
- 32: **end for**

Once the access network is planned, the wireless BH links are determined based on the maximum received power from candidate BH nodes having LOS. Candidate MCs are prioritized over SCs since the former implies direct links. In addition, SCs backhauled by another SC cannot serve as BH node because of the multi-hop constraint in Equation (13). It is possible that some SCs cannot have a LOS BH link from their location or that the condition in Equation (14) is not met. In these cases, Algorithm 2 is executed to make the BH-aware optimization process. The algorithm starts by modifying the candidate SC location in case of NLOS. Specifically, Steps 1–10 replace the infeasible location by a new location having LOS to the BH node that minimizes the distance between both locations. Since there is an initial set of deployed nodes, a valid location with LOS can be found out for backhauling any SC. Then, if an SC exceeds the maximum number of backhauled SCs, Steps 11–32 aim at finding another alternative for each backhauled SC until the constraint in Equation (14) is met. The location of these SCs can be modified to have LOS to the newly assigned BH node. The selection of the SCs to satisfy the constraint in Equation (14) is based on the minimum displacement to have a LOS position. Given that the MCs are not limited by the number of backhauled SCs, the algorithm will provide a solution that satisfies the constraint in Equation (14) at any case.

4. Performance Evaluation

4.1. Simulation Scenario and Setup

The simulated scenario covers an urban area of 1 km × 1 km with a set of deployed MCs and SCs, which are located according to the spatial variations of the traffic demand. The deployment scenario is simulated following a snapshot-based model, where each snapshot involves a random realization of the same traffic probability distribution. The evaluation of a wide range of different situations ensures reliable statistical significance analysis. Let us assume that the expansion of a certain tenant's service results in a lack of capacity with the current infrastructure. The UE demand is randomly and non-uniformly distributed over the considered area. The configured UE service demand (20 Mbps) is representative for average human mobile or nomadic applications in busy hours, provided that virtual reality and high-definition video are among the most typical 5G mobile broadband services. With respect to the BH network, the antenna main-lobe width θ^m is set to 10° and the gains A_{max} and A_{min} are set to 12 and -2 dBi, respectively, unless stated otherwise [35]. The cell bandwidth W^{BH} in the BH is fixed to 1 GHz, and it does not interfere with the access spectrum. Regarding the proposed algorithm, $N_S = 2$ is set to limit the required capacity per BH link, $\alpha = 0.7$ allows partial service degradation and $\beta = 0.8$ allows small congestion in BH links. The other relevant simulation parameters are shown in Table 1.

Table 1. Simulation parameters for access and BH networks.

Parameter	Access	BH
Operating frequency (GHz)	MC: 5 SC: 60	60
Cell bandwidth (MHz)	MC: 100 SC: 250–1000	1000
Propagation—path loss	3GPP model [36]	3GPP model [36]
MC antenna gain (dBi)	12	[12–25]
SC antenna gain (dBi)	10	[12–25]
MC transmit power (dBm)	43	33
SC transmit power (dBm)	25–33	30
Antenna height (m)	UE: 1.5, MC: 25, SC: 12	MC: 25, SC: 12
UE service demand (Mbps)	20	-
Number of demand realizations	100	100

As a reference for comparison, several methods are considered in the evaluation. Since solving the formulated problem requires impractical computational time, the optimal solution is approximated through a combination of exhaustive search and heuristic strategy. In particular, an exhaustive-search BH-aware (ESBA) and an exhaustive-search ideal-BH (ESIB) dimensioning and planning algorithms are developed following the same principles as in [16,32]. Specifically, the SCs are iteratively added one by one in locations that are selected by brute-force from the set of candidate locations to maximize the spectral efficiency in the access. In ESBA, the candidate locations are those having LOS BH and satisfying the BH-related constraints in Equations (12)–(17). The ESIB algorithm, which does not consider these constraints, serves to establish an upper-bound on the performance for the non-ideal BH scenario. In addition to these methods, a random-selection BH-aware (RSBA) dimensioning and planning algorithm is developed to establish an approximation lower-bound. In this case, the SCs are iteratively added one by one in random locations that satisfy the BH-related constraints.

The experiments were conducted on a Windows 10 desktop machine featuring an Intel Core i7-6700 @ 3.40 GHz CPU and 8.00 GB RAM.

4.2. Simulation Results and Discussions

Figure 1 represents the deployment scenario resulting from applying each planning algorithm to support a total traffic demand of 5 Gbps. The colored contour lines indicate the traffic demand density. The dots represent the UE locations for a certain realization of the statistical distribution of the traffic

demand. In the four cases, the algorithm starts from an initial set of deployed nodes, marked with blue triangles, which were derived from previous planning stage(s). The newly planned SCs are represented by red triangles. The grey lines indicate the BH links between nodes, except for ESIB where the BH is ideal (i.e., BH constraints are not considered). For CEBA, ESBA and ESIB, it is observed that the regions with higher traffic densities are covered by a larger number of SCs. In the case of CEBA and ESBA, these SCs are optimally placed to both increase resource usage efficiency and support BH links with LOS and complying with the maximum number of backhauled SCs and multi-hops. Additionally, it is observed that ESBA exhibits a lower cell density (or larger cell service areas) in low traffic regions than CEBA. Looking at the RSBA deployment, it is noted that the SCs are randomly placed in locations where the BH link is ensured, without keeping a relationship with the traffic demand.

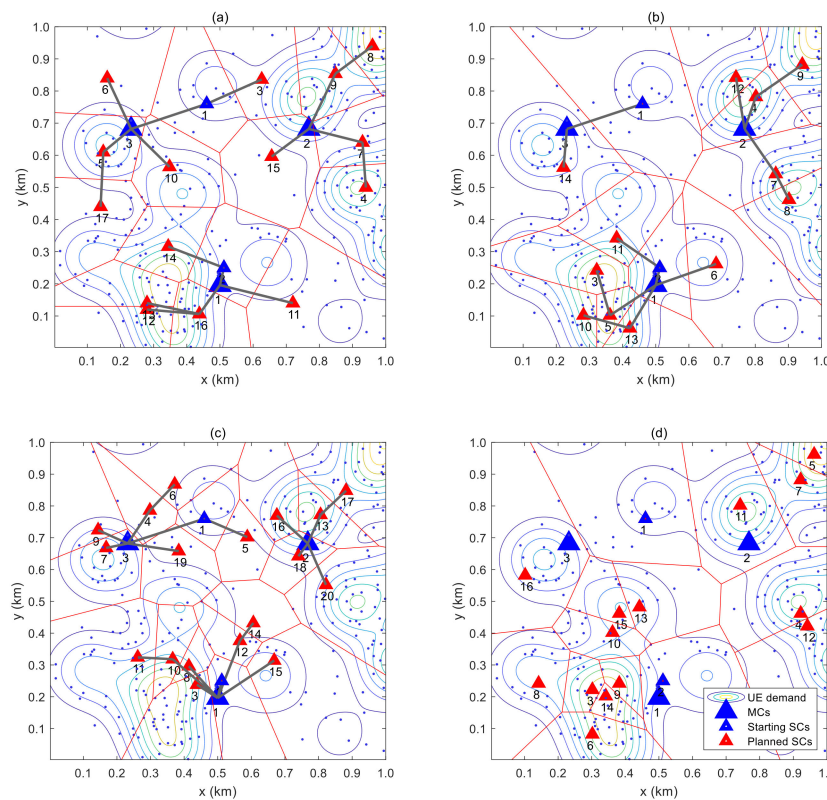


Figure 1. Example network deployment for a traffic demand of 5 Gbps in the overall area for each evaluated algorithm. (a) CEBA method; (b) ESBA method; (c) RSBA method; (d) ESIB method.

Figure 2 compares the performance of the four algorithms. In particular, the number of planned SCs and the average spectral efficiency in the access network are shown for different MC densities and different magnitudes of the traffic demand. Varying the MC density serves to establish different BH conditions, while varying the traffic demand allows analyzing capacity issues in the scenario. As expected, RSBA and ESIB establish lower and upper bounds, respectively, on the level of performance reachable by the methods. The optimal method, ESBA, approximates the performance of ESIB as the MC density increases, showing that the BH constraints are less relevant for higher densities. In particular, for 2 MCs/km², the impact of the BH network is appreciable on both indicators by comparing ESBA with ESIB. To understand the increased number of SCs, note that the distance between MCs and SCs is limited by the maximum allowed path loss. Consequently, for a low number of MCs in the scenario, multi-hop BH links may frequently be required to reach distant areas, increasing the number of SCs. For 3 MCs/km², the BH impact is appreciable on the spectral efficiency and insignificant on the number of SCs. Since in this case there are more locations satisfying the LOS condition, multi-hop BH links are less probable. Thus, ESBA approximates the same number of SCs as in the ideal case given by

ESIB. However, deviations from the optimal location due to the BH constraints still impact the spectral efficiency as shown in Figure 2d.

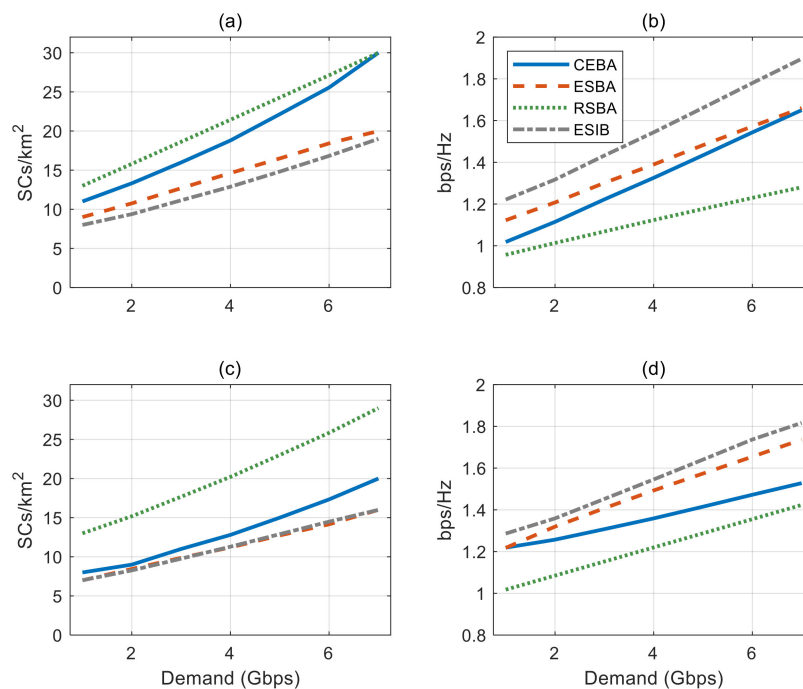


Figure 2. Performance comparison in terms of number of SCs (#SCs) and spectral efficiency for different MC densities and traffic demands. (a) #SCs for 2 MCs/km²; (b) Spectral efficiency for 2 MCs/km²; (c) #SCs for 3 MCs/km²; (d) Spectral efficiency for 3 MCs/km².

The proposed method, CEBA, is more sensitive to the BH conditions than ESBA. For 2 MCs/km², CEBA increases the number of SCs, on average, by 26% in comparison with ESBA. Such an increase is accentuated for higher traffic demands. Looking at the spectral efficiency, as the traffic demand increases, CEBA approaches the ESBA's curve as a consequence of the increasing number of deployed SCs. This behavior of CEBA changes drastically for MC densities above 2 MCs/km². Specifically, for 3 MCs/km² and low-medium traffic demands, the number of SCs is only increased by 10% compared to ESBA (and ESIB). It also deviates significantly from the random case. This is due to the smaller distances between MCs and SCs, which minimize the SC relocations made by CEBA.

For high traffic demands (above 5–6 Gbps), the slope of the CEBA's curve representing the number of SCs experiences a moderate increase. This effect is appreciable for the two values of MC densities shown in Figure 2. This is mainly because of the presence of BH links with insufficient capacity to meet the demand (e.g., due to traffic aggregation in multi-hop BH links), even though the LOS condition is satisfied. To explain this, consider the access and BH capacity conditions (Equations (11) and (12), respectively), which take part in the main loop of CEBA's Algorithm 1. It is observed (not shown for brevity) that the first iterations of this loop are triggered by breaking Equation (11), while the last iterations are triggered by breaking Equation (12). Since the bandwidth in the BH is not modified, the only solution is to increase the number of SCs to distribute the access demand among more BH links until Equation (12) is satisfied. This issue can also be solved by increasing the antenna gain as discussed in the next paragraph.

To study the effect of the directional high-gain and narrow-beam antennas on BH network performance, three different values of the antenna gain are evaluated for the scenario with 3 MCs/km² and CEBA planning method. Figure 3 shows the number of planned SCs and the average spectral efficiency measured in the BH network. It is observed that, for high traffic demands, the number of planned SCs is smaller for 18 and 25 dBi gains. This is due to an increase of about 1 bps/Hz in the

spectral efficiency, as shown in Figure 3b. In particular, when the BH capacity condition defined in Equation (12) is checked in the main loop of CEBA's Algorithm 1, it returns a true value, indicating that the BH links are not congested and, therefore, additional SCs are not needed. The improvement in the average spectral efficiency is more pronounced in the range of low-to-medium values of the antenna gain. Accordingly, 18 dBi gain provides a good trade-off between spectral efficiency and antenna complexity.

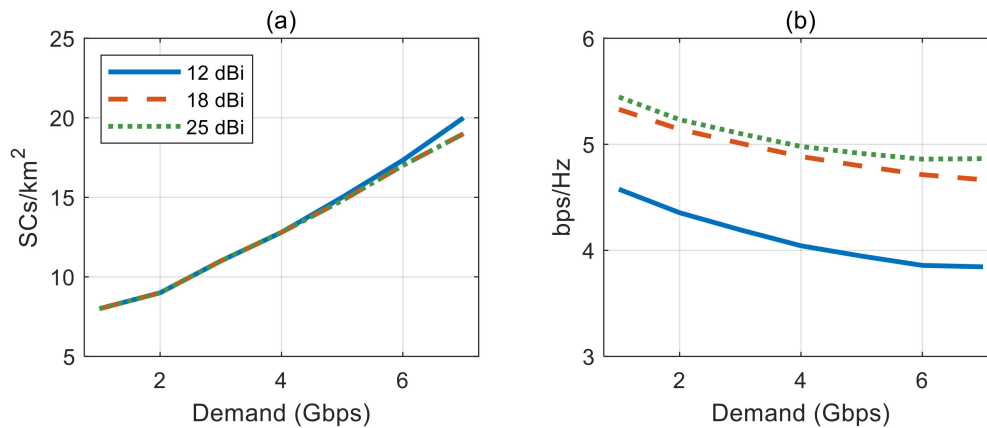


Figure 3. Evaluation in terms of number of SCs (#SCs) and spectral efficiency in the BH network for different values of the antenna gain. (a) #SCs; (b) BH spectral efficiency.

Table 2 shows a comparison of the planning algorithms in terms of computational complexity. Specifically, it provides the simulation time of each method for different traffic demands and an MC density of 2 MCs/km². In general, this time increases with the traffic demand since more iterations are required to place additional SCs. Looking at the differences between methods, RSBA gives the lowest values since it follows a very simple logic for cell planning. Consequently, most of the simulation time is spent in network performance computation. The proposed method, CEBA, increases the simulation time with respect to RSBA by a factor of 2–3. This increment is mainly determined by the execution of the *k*-means, the steepest-ascent and the BH-aware optimization algorithms. Nevertheless, such an increase factor reveals a good trade-off between complexity and effectiveness of the solution. On the contrary, ESBA and ESIB provide the greatest values of the simulation time due to the high computational load of the exhaustive search approach. In particular, the increase factors are 25–37, which are considerably higher than those obtained by CEBA. Contrary to expectations, ESIB achieves larger simulation times than ESBA even though the BH network is not simulated. The underlying reason is that the set of candidate solutions that are evaluated by brute-force in the case of ESBA is smaller due to the required LOS condition.

Table 2. Measured simulation time in minutes for the methods.

Method	Traffic Demand [Gbps]			
	1.0	3.0	5.0	7.0
CEBA	13.6	41.0	56.3	197.5
ESBA	123.1	381.7	813.2	1444.3
RSBA	4.1	12.3	30.5	53.9
ESIB	150.0	419.4	771.1	1709.4

The simulation time is also impacted by the scenario size and the grid size, since they determine the number of candidate locations. The required computation resources for exhaustive-search methods such as ESBA and ESIB represent a bottleneck, as their scalability is very limited when large-scale

scenarios are considered. Thus, the benefits of using computationally-efficient methods such as CEBA are very valued.

5. Conclusions

In this work, the authors propose a computationally-efficient algorithm for the dimensioning and planning of SCs under non-ideal BH conditions. The main contributions to this field rely on the consideration of a set of constraints in the BH that limit the location of the SCs, which are deployed on top of an existing HetNet infrastructure that is available to support the deployment of the new SCs. Specifically, the algorithm defines two phases to first determine a candidate solution that satisfies the user demand and then modify the solution to meet the BH constraints. Since some SCs may not have a LOS BH link from their initial candidate location, the BH-aware optimization modifies such locations based on the minimum displacement to have a LOS position. Simulation results show that, for sufficient MC density and low-medium traffic demands, the performance of the solution in terms of number of deployed SCs approximates those obtained by exhaustive-search methods, using much less computational resource.

Author Contributions: Conceptualization, P.M.; Formal analysis, P.M. and P.A.; Investigation, P.M., O.A.-H., P.A. and J.J.R.-M.; Methodology, O.A.-H. and P.A.; Resources, J.N.-O. and J.J.R.-M.; Software, J.N.-O. and J.J.R.-M.; Validation, O.A.-H. and J.N.-O.; Writing—original draft, P.M. and O.A.-H.; Writing—review & editing, P.A., J.N.-O. and J.J.R.-M. All authors have read and agreed to the published version of the manuscript.

Funding: This work was partially supported by the H2020 research and innovation project 5G-CLARITY (Grant No. 871428) and by the Spanish Ministry of Science, Innovation and Universities (project PID2019-108713RB-C53).

Conflicts of Interest: The authors declare no conflict of interest.

References

1. Mitra, R.N.; Agrawal, D.P. 5G mobile technology: A survey. *Ict Express* **2015**, *1*, 132–137. [[CrossRef](#)]
2. Siddiqi, M.A.; Yu, H.; Joung, J. 5G Ultra-Reliable Low-Latency Communication Implementation Challenges and Operational Issues with IoT Devices. *Electronics* **2019**, *8*, 981. [[CrossRef](#)]
3. GSMA. Road to 5G Introduction and Migration. In *White Paper*; GSM Association: London, UK, 2018; Available online: https://www.gsma.com/futurenetworks/wp-content/uploads/2018/04/Road-to-5G-Introduction-and-Migration_FINAL.pdf (accessed on 23 August 2020).
4. GSMA. Mobile backhaul options. Spectrum analysis and recommendations. In *White Paper*; GSM Association: London, UK, 2018; Available online: <https://www.gsma.com/spectrum/wp-content/uploads/2019/04/Mobile-Backhaul-Options.pdf> (accessed on 23 August 2020).
5. Xiao, K.; Li, W.; Kadoch, M.; Li, C. On the Secrecy Capacity of 5G MmWave Small Cell Networks. *IEEE Wirel. Commun.* **2018**, *25*, 47–51. [[CrossRef](#)]
6. Okasaka, S.; Weiler, R.J.; Keusgen, W.; Pudseyev, A.; Maltsev, A.; Karls, I.; Sakaguchi, K. Proof-of-Concept of a Millimeter-Wave Integrated Heterogeneous Network for 5G Cellular. *Sensors* **2016**, *16*, 1362. [[CrossRef](#)] [[PubMed](#)]
7. Rezaabad, A.L.; Beyranvand, H.; Salehi, J.A.; Maier, M. Ultra-Dense 5G Small Cell Deployment for Fiber and Wireless Backhaul-Aware Infrastructures. *IEEE Trans. Veh. Technol.* **2018**, *67*, 12231–12243. [[CrossRef](#)]
8. Feng, W.; Li, Y.; Jin, D.; Su, L.; Chen, S. Millimetre-Wave Backhaul for 5G Networks: Challenges and Solutions. *Sensors* **2016**, *16*, 892. [[CrossRef](#)] [[PubMed](#)]
9. Saha, C.; Dhillon, H.S. Millimeter Wave Integrated Access and Backhaul in 5G: Performance Analysis and Design Insights. *IEEE J. Sel. Areas Commun.* **2019**, *37*, 2669–2684. [[CrossRef](#)]
10. Song, X.; Hälsig, T.; Cvetkovski, D.; Rave, W.; Lankl, B.; Grass, E.; Fettweis, G. Design and Experimental Evaluation of Equalization Algorithms for Line-of-Sight Spatial Multiplexing at 60 GHz. *IEEE J. Sel. Areas Commun.* **2018**, *36*, 2570–2580. [[CrossRef](#)]
11. Chataut, R.; Akl, R. Massive MIMO Systems for 5G and beyond Networks—Overview, Recent Trends, Challenges, and Future Research Direction. *Sensors* **2020**, *20*, 2753. [[CrossRef](#)] [[PubMed](#)]
12. Gkonis, P.K.; Trakadas, P.T.; Kaklamani, D.I. A Comprehensive Study on Simulation Techniques for 5G Networks: State of the Art Results, Analysis, and Future Challenges. *Electronics* **2020**, *9*, 468. [[CrossRef](#)]

13. Busari, S.A.; Huq, K.M.S.; Mumtaz, S.; Dai, L.; Rodriguez, J. Millimeter-Wave Massive MIMO Communication for Future Wireless Systems: A Survey. *IEEE Commun. Surv. Tutor.* **2018**, *20*, 836–869. [[CrossRef](#)]
14. Ghazzai, H.; Yaacoub, E.; Alouini, M.S.; Dawy, Z.; Abu-Dayya, A. Optimized LTE cell planning with varying spatial and temporal user densities. *IEEE Trans. Veh. Technol.* **2016**, *65*, 1575–1589. [[CrossRef](#)]
15. Yaacoub, E.; Dawy, Z. LTE radio network planning with HetNets: BS placement optimization using simulated annealing. In Proceedings of the 17th IEEE Mediterranean Electrotechnical Conference, Beirut, Lebanon, 13–16 April 2014; pp. 327–333. [[CrossRef](#)]
16. Son, K.; Oh, E.; Krishnamachari, B. Energy-efficient design of heterogeneous cellular networks from deployment to operation. *Comput. Netw.* **2015**, *78*, 95–106. [[CrossRef](#)]
17. Ganame, H.; Yingzhuang, L.; Ghazzai, H.; Kamissoko, D. 5G Base Station Deployment Perspectives in Millimeter Wave Frequencies Using Meta-Heuristic Algorithms. *Electronics* **2019**, *8*, 1318. [[CrossRef](#)]
18. Athanasiadou, G.E.; Fytampanis, P.; Zarbouti, D.A.; Tsoulos, G.V.; Gkonis, P.K.; Kklamani, D.I. Radio Network Planning towards 5G mmWave Standalone Small-Cell Architectures. *Electronics* **2020**, *9*, 339. [[CrossRef](#)]
19. Soorki, M.N.; Saad, W.; Bennis, M. Optimized Deployment of Millimeter Wave Networks for In-Venue Regions with Stochastic Users' Orientation. *IEEE Trans. Wirel. Commun.* **2019**, *18*, 5037–5049. [[CrossRef](#)]
20. Tonini, F.; Fiorani, M.; Raffaelli, C.; Wosinska, L.; Monti, P. Benefits of joint planning of small cells and fiber backhaul in 5G dense cellular networks. In Proceedings of the IEEE International Conference on Communications (ICC), Paris, France, 21–25 May 2017; pp. 1–6. [[CrossRef](#)]
21. Xu, X.; Saad, W.; Zhang, X.; Xu, X.; Zhou, S. Joint Deployment of Small Cells and Wireless Backhaul Links in Next-Generation Networks. *IEEE Commun. Lett.* **2015**, *19*, 2250–2253. [[CrossRef](#)]
22. Mesodiakaki, A.; Kassler, A.; Zola, E.; Ferndahl, M.; Cai, T. Energy efficient line-of-sight millimeter wave small cell backhaul: 60, 70, 80 or 140 GHz? In Proceedings of the IEEE 17th International Symposium on A World of Wireless, Mobile and Multimedia Networks (WoWMoM), Coimbra, Portugal, 21–24 June 2016; pp. 1–9. [[CrossRef](#)]
23. Bonfante, A.; Giordano, L.G.; López-Pérez, D.; Garcia-Rodriguez, A.; Geraci, G.; Baracca, P.; Butt, M.M.; Marchetti, N. 5G Massive MIMO Architectures: Self-Backhauled Small Cells Versus Direct Access. *IEEE Trans. Veh. Technol.* **2019**, *68*, 10003–10017. [[CrossRef](#)]
24. Kwon, G.; Park, H. Joint User Association and Beamforming Design for Millimeter Wave UDN with Wireless Backhaul. *IEEE J. Sel. Areas Commun.* **2019**, *37*, 2653–2668. [[CrossRef](#)]
25. Łukowa, A.; Venkatasubramanian, V. Dynamic In-band Self-backhauling for 5G Systems with Inter-Cell Resource Coordination. *Int. J. Wirel. Inf. Netw.* **2019**, *26*, 319–330. [[CrossRef](#)]
26. Saadat, S.; Chen, D.; Jiang, T. Multipath multihop mmWave backhaul in ultra-dense small-cell network. *Digit. Commun. Netw.* **2018**, *4*, 111–117. [[CrossRef](#)]
27. Tran, G.K.; Santos, R.; Ogawa, H.; Nakamura, M.; Sakaguchi, K.; Kassler, A. Context-Based Dynamic Meshed Backhaul Construction for 5G Heterogeneous Networks. *J. Sens. Actuator Netw.* **2018**, *7*, 43. [[CrossRef](#)]
28. Marabissi, D.; Fantacci, R.; Simoncini, L. SDN-Based Routing for Backhauling in Ultra-Dense Networks. *J. Sens. Actuator Netw.* **2019**, *8*, 23. [[CrossRef](#)]
29. Semiari, O.; Saad, W.; Bennis, M.; Dawy, Z. Inter-Operator Resource Management for Millimeter Wave Multi-Hop Backhaul Networks. *IEEE Trans. Wirel. Commun.* **2017**, *16*, 5258–5272. [[CrossRef](#)]
30. Almohamad, A.; Hasna, M.O.; Khattab, T.; Haouari, M. An Efficient Algorithm for Dense Network Flow Maximization with Multihop Backhauling and NFPs. In Proceedings of the IEEE 90th Vehicular Technology Conference (VTC2019-Fall), Honolulu, HI, USA, 22–25 September 2019; pp. 1–5. [[CrossRef](#)]
31. Hong, J.; Park, J.; Beak, S. Millimeter-Wave-Based Cooperative Backhaul for a Mobile Station in an X-Haul Network. *IEEE Syst. J.* **2019**, *13*, 2500–2506. [[CrossRef](#)]
32. Muñoz, P.; Sallent, O.; Pérez-Romero, J. Self-Dimensioning and Planning of Small Cell Capacity in Multitenant 5G Networks. *IEEE Trans. Veh. Technol.* **2018**, *67*, 4552–4564. [[CrossRef](#)]
33. Quadri, C.; Premoli, M.; Ceselli, A.; Gaito, S.; Rossi, G.P. Optimal Assignment Plan in Sliced Backhaul Networks. *IEEE Access* **2020**, *8*, 68983–69002. [[CrossRef](#)]
34. 3GPP. *Study on New Radio Access Technology: Radio Frequency (RF) and Co-existence Aspects*, version 14.2.0; TR 38.803; European Telecommunications Standards Institute: Valbonne, France, 2017.
35. Singh, S.; Kulkarni, M.N.; Ghosh, A.; Andrews, J.G. Tractable Model for Rate in Self-Backhauled Millimeter Wave Cellular Networks. *IEEE J. Sel. Areas Commun.* **2015**, *33*, 2196–2211. [[CrossRef](#)]

36. 3GPP. *Study on Channel Model for Frequencies from 0.5 to 100 GHz*, version 15.0.0; TR 38.901; European Telecommunications Standards Institute: Valbonne, France, 2018.
37. Yuan, Y. *LTE-Advanced Relay Technology and Standardization*; Springer: Berlin/Heidelberg, Germany, 2013.
38. Ju, S.; Rappaport, T.S. Simulating Motion-Incorporating Spatial Consistency into NYUSIM Channel Model. In Proceedings of the IEEE 88th Vehicular Technology Conference (VTC-Fall), Chicago, IL, USA, 27–30 August 2018; pp. 1–6. [[CrossRef](#)]
39. Hilt, A. Availability and Fade Margin Calculations for 5G Microwave and Millimeter-Wave Anyhaul Links. *Appl. Sci.* **2019**, *9*, 5240. [[CrossRef](#)]



© 2020 by the authors. Licensee MDPI, Basel, Switzerland. This article is an open access article distributed under the terms and conditions of the Creative Commons Attribution (CC BY) license (<http://creativecommons.org/licenses/by/4.0/>).